

## {311} facets of selectively grown epitaxial Si layers on SiO<sub>2</sub>-patterned Si(100) surfaces

Hiroyuki Hirayama, Masayuki Hiroi, and Takashi Ide

*Microelectronics Research Laboratories, NEC Corporation, 34 Miyukigaoka, Tsukuba 305, Japan*

(Received 21 June 1993)

A Si epitaxial layer was selectively grown on SiO<sub>2</sub>-patterned Si(100) with no miscut and on 1°, 3°, and 4° miscut vicinal surfaces by ultrahigh-vacuum chemical-vapor deposition using disilane. On the patterned Si(100) surfaces with and without miscuts, faceted (100) layers grew. Although {111} is energetically the most stable surface, the resulting facets had {311} orientation. This means that the {311} faceting is related to the growth kinetics rather than the energetics. Macroscopically, the {311} faceting is caused by the slower growth rate of the (311) surface than that of the (100) surface. On the vicinal surfaces, the top surface of the selectively grown layer was not vicinal but had exactly (100) orientation. This indicates the ready incorporation of adatoms into the step edges of (100) terraces and the subsequent step-flow growth mode. When the flowing step reaches the end of the top surface, it is swallowed into the facet and disappears. This decreases the step density and makes the vicinal surface flat. With respect to the swallowing of the growing steps at the facet corner, we propose a microscopic model for the {311} faceting.

### I. INTRODUCTION

Selective epitaxial growth of Si and Si<sub>1-x</sub>Ge<sub>x</sub> on SiO<sub>2</sub> patterned Si substrates can be accomplished by ultrahigh-vacuum chemical vapor deposition (UHV-CVD) using gaseous sources such as disilane and germane.<sup>1-3</sup> Epitaxial layers self-aligned to the SiO<sub>2</sub> pattern are automatically obtained by this method; this is a highly advantageous feature for ultralarge-scale integrated (ULSI) device fabrication.<sup>4</sup> However, facets always appear at the boundary between the Si layer and the SiO<sub>2</sub> side wall. From the viewpoint of device application, this is a severe problem because the facet makes an exposed empty space at the SiO<sub>2</sub> pattern edge and causes an inactive device area along the SiO<sub>2</sub> sidewall boundary.

To suppress faceting, we believe that an understanding of the faceting mechanism is necessary. Basically, faceting occurs to reduce excess energy of the interface between the epitaxially grown layer and the SiO<sub>2</sub> side wall.<sup>5</sup> If the epitaxial layer grows close to the SiO<sub>2</sub> sidewall, all the atoms at the sidewall boundary have dangling bonds toward the SiO<sub>2</sub>. To reduce the energy of these dangling bonds, the epitaxial layer makes a facet with a smaller surface energy. However, the surface with the lowest surface energy does not necessarily appear as the facet. A typical example is the selective epitaxial growth of Si on a SiO<sub>2</sub> patterned Si(100) surface. Although Si{111} has the lowest surface energy,<sup>6</sup> we reported here than not {111} but {311} facets are always observed in selective epitaxial growth on Si(100). {311} facets are also observed for Si epitaxial layers on Si surfaces,<sup>7-9</sup> Ge epitaxial layer on Si(100),<sup>10</sup> and Si<sub>1-x</sub>Ge<sub>x</sub> alloy on Si(100) surface.<sup>11,12</sup> Hence, the {311} facet seems to be a general feature of column-IV semiconductor crystal growth. However, even if surface reconstructions are considered, recent first-principle calculations have indicated that the surface energy of Si{311} is larger than both Si{111} and

Si{100}.<sup>13</sup> This suggests that the appearance of the {311} facet is related to growth kinetics. In this paper, facet formation of selectively grown Si layers on exactly cut Si(100) and Si(100) 1°, 3°, and 4° vicinal surfaces is presented. On all surfaces, {311} facets were observed. The measured growth rates on {100}, {311}, and {111} surfaces indicate that the {311} facet is related to the growth kinetics. Moreover, on Si(100) vicinal surfaces, the top surface orientation of the grown layer changes from Si(100) vicinal to exactly Si(100). This is due to the ready incorporation of Si adatoms at the step edge, and the resulting step-flow motion toward the facet. With respect of the facet growth due to the step swallowing at the boundary between the top (100) surface and the facet surface, a model for the {311} faceting is proposed.

### II. EXPERIMENT

Four-inch Si(100) wafers with miscut of 0°, 1°, 3°, and 4° having a SiO<sub>2</sub> pattern of 1000-Å thermal oxide were used as substrates. On these substrates, selective epitaxial growth of Si layers was achieved using UHV-CVD.<sup>3</sup> The base pressure of the growth chamber was less than 5×10<sup>-9</sup> Torr. For Si epitaxial growth, disilane was introduced into the chamber. The flow rate of disilane was 1 standard cubic cm per minute (sccm). The pressure during growth was 1×10<sup>-5</sup> Torr, and substrate temperature was kept at 550°C. The film thickness was proportional to the growth time. Selectively grown Si layers were produced on the Si window areas on the patterned substrates. Perfect selectivity was confirmed *in situ* by the lack of a ringlike reflection high-energy electron diffraction (RHEED) pattern from polycrystalline Si on the SiO<sub>2</sub> area. The selectivity was also confirmed *ex situ* by secondary electron microscopy (SEM). The crystal shape of the selectively grown layers was observed by cross-sectional SEM images.

Besides the facet observation, the growth rates were in-

dependently measured at the substrate temperature of 550°C on Si(100), (311), and (111) surfaces. Here, the growth rate was determined as a function of the disilane flow rate. On the SiO<sub>2</sub> patterned 4-in. wafers, Si epitaxial layers were selectively grown. The thickness of the selectively grown layer was measured by taristep after removing the SiO<sub>2</sub> pattern with HF solution. The growth rate was obtained using the thickness and the growth time.

### III. RESULTS

Typical crystals of the selectively grown Si layer on the Si(100) surface with no miscut are shown in Fig. 1. The (100) top layer and facet surfaces are observed with the angle between (100) and the facet indicating that the facet orientation is {311}. With further growth, the facets become dominant, finally resulting in a triangular shape with two {311} facets, as in Fig. 2. As described in the Introduction, an orientation of low surface energy is generally favorable for a facet. Among Si low-index surfaces, {111} has the lowest surface energy, whereas {311} is metastable.<sup>6</sup> Hence, thermodynamically, {311} facet formation is difficult to understand.

Very recently, Eaglesham *et al.*<sup>6</sup> pointed out that, if {311} has a small but finite cusp in surface energy as a function of surface orientation, the {311} facet has a chance to appear to make a transition from convex to concave shape at the island edge, since Si is constrained to have zero contact angle with Si. In thermally non-equilibrium growth phenomena, this may strongly favor the facet of a small contact angle; {311}.<sup>6</sup> But, as shown in Fig. 2, {311} faceting continued until the (100) top surface disappeared. This cannot be understood from the viewpoint of a contact angle. The result of Fig. 2 suggests that the {311} facet is automatically built in during growth.

Figure 3 shows results of Si selective epitaxial growth on Si(100) 1°, 3°, and 4° miscut substrates. In each case, {311} facets were observed at the SiO<sub>2</sub> boundary. However, the top surface of the selectively grown layer was found to form an exact Si(100) surface; i.e., the top sur-

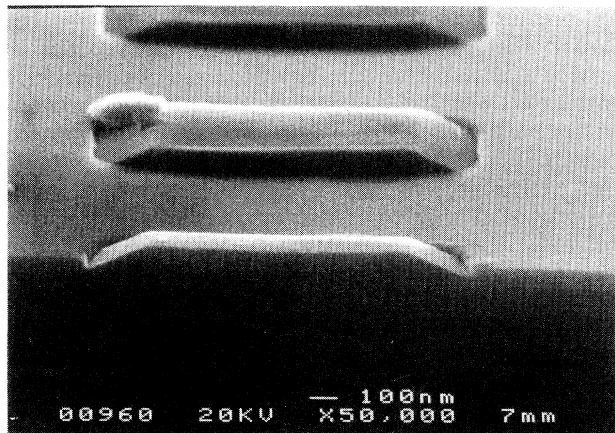


FIG. 1. SEM image of a selectively grown Si layer on the SiO<sub>2</sub> patterned Si(100) surface with no miscut.

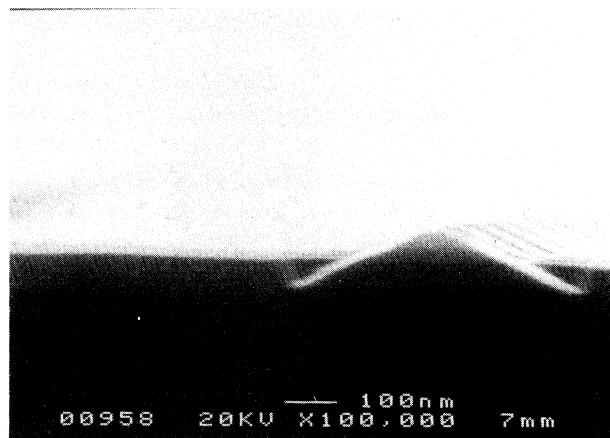


FIG. 2. SEM image of a selectively grown Si layer on the SiO<sub>2</sub> patterned Si(100) surface with no miscut, in which the {311} facets grew until the top (100) surface disappeared.

face of the layer changes from Si(100) vicinal to exactly Si(100) during growth, as illustrated in Fig. 4. As will be discussed in the next section, this observed change is caused by swallowing of the steps at the facet boundary.

### IV. DISCUSSION

#### A. {311} facet

In this section, we discuss the {311} faceting with respect to the relative growth rates of Si(100), (311), and (111) surfaces. But before discussing the special situation of {311} facets, we summarize general features of facet growth, schematically illustrated in Fig. 5. In this figure, we assume that the growth rate of the top surface "A" is larger than that of the facet surface "B." During growth, Si impinges on both surfaces; Si adsorbed on "A" causes the growth of the top surface indicated by the arrow "a." whereas Si adsorbed on "B" causes the growth of the facet indicated by the arrow "b." However, notice that growth of the facet toward arrow "c" is not caused by growth of the facet surface, but by nucleation at the corner point "P" of the Si adsorbed on the top surface. In our growth on SiO<sub>2</sub> patterned Si(100) substrates, the top surface was (100) oriented. On Si(100), Si growth by UHV-CVD proceeds via a layer-by-layer mode.<sup>1,12</sup> Hence, facet growth proceeds via step nucleation at the corner point "P." And, as a result, the facet surface of lower growth rate expands by swallowing (100) terraces.

The Si epitaxial growth rate depends on the substrate orientation. The growth rates on Si(100), (311), and (111) surfaces are indicated as a function of the disilane flow rate in Fig. 6. As shown in the figure, the growth rate initially increases with the disilane flow rate on all the surfaces. But, at large flow rates, it seems to be saturated. The initial increase and the following saturation of the growth rate are characteristic of the UHV-CVD growth.<sup>1</sup> In UHV-CVD, the disilane source gas molecule dissociatively adsorbs on the surface dangling bond. The resulting SiH fragment occupies the surface dangling-bond site,

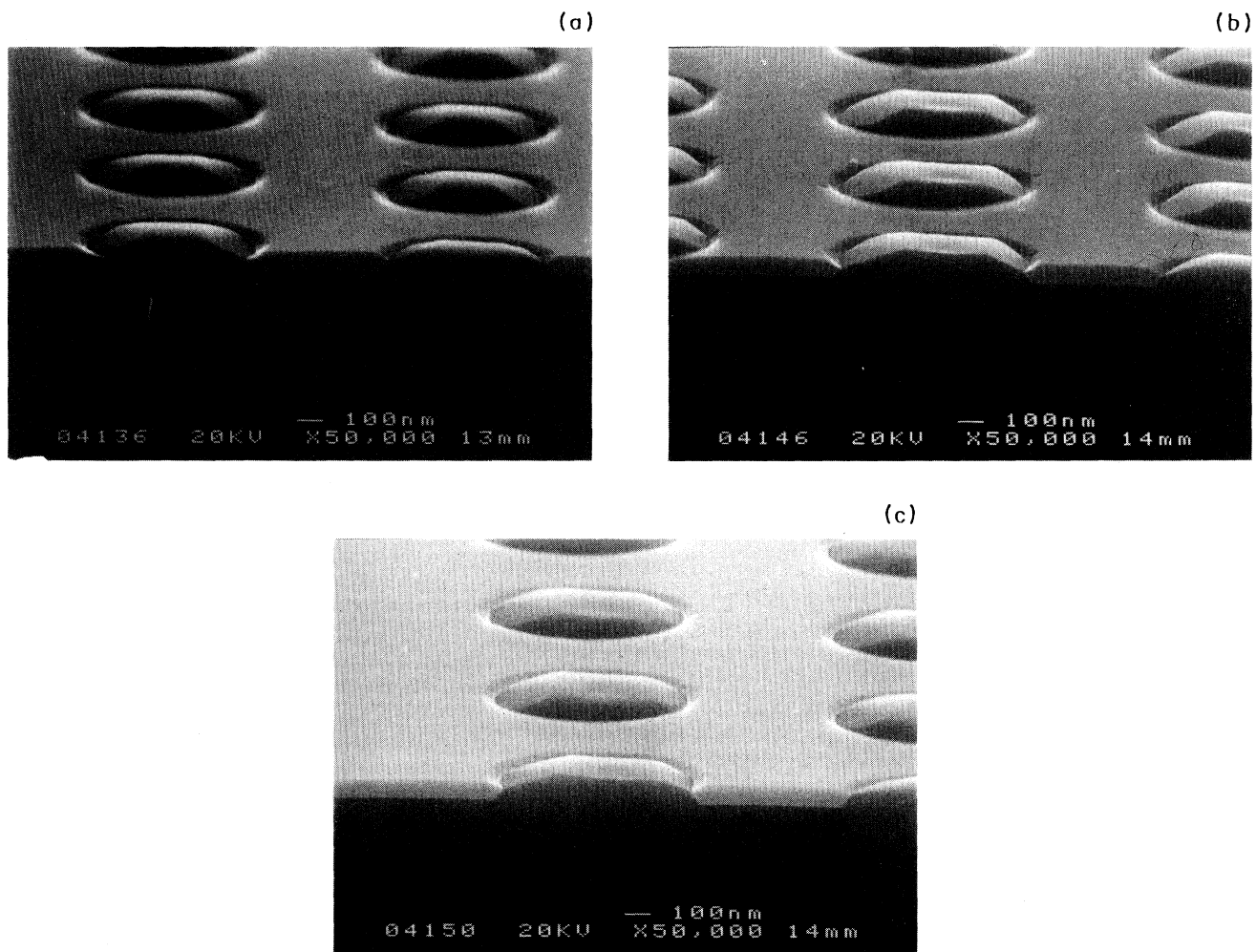


FIG. 3. SEM images of selectively grown Si layers on  $\text{SiO}_2$  patterned Si(100) vicinal surfaces with miscut angles of (a)  $1^\circ$ , (b)  $3^\circ$ , and (c)  $4^\circ$  off.

and then the H thermally desorbs. After the H desorption, a fresh dangling bond appears on the newly grown surface, on which the dissociative adsorption of disilane is repeated, and the growth proceeds.<sup>1</sup> Within the framework of this growth mechanism, the growth rate is determined by the balance between the impinging disilane flux and the H desorption rate. At a large flow rate, H

desorption rate is slower than the disilane impinging rate. In this case, most of the surface dangling bond is saturated by the H during the growth, and the growth rate is limited by the thermal-desorption rate of H. This makes the growth rate independent of the disilane flow rate. But with a small flow rate, the impinging rate of disilane is slower than the H desorption rate. In this case, there are

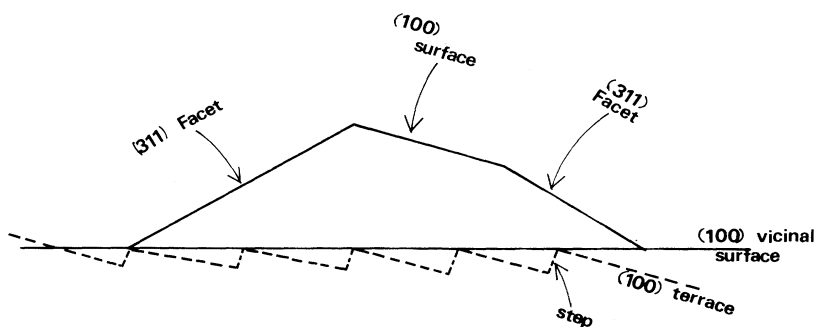


FIG. 4. Sketch of selectively grown Si layers on a  $\text{SiO}_2$  patterned Si(100) vicinal surface. The broken line indicates that the vicinal surface is constructed by (100) terraces and steps.

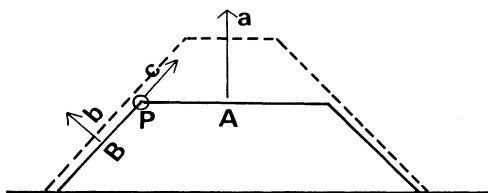


FIG. 5. Schematic illustration of faceted layer growth. The top layer "A" is assumed to have a higher growth rate than the facet surface "B." "P" is the corner point between the top and facet surfaces. Vectors represents growth rates.

still many surface dangling bonds which are available for the dissociative adsorption of disilane molecule. Here, the growth rate is proportional to the flow rate. Therefore, the growth rate increases with the flow rate and is then saturated, as shown in Fig. 6. Because the sticking coefficient of disilane and the H desorption rate depend on the surface orientation, the growth rate also depends on the surface orientation.

In our facet study, Si layers were grown with a small flow rate of 1 sccm, where the growth rates on Si(100), (311), and (111) are 40, 100, and 170 Å/min, respectively. Hence, in the growth on Si(100), both {311} and {111} can grow as a dominant facet because of their slower growth rate. However, if both {311} and {111} had an even chance to form a facet surface, during growth the {111} facet would be larger than the {311} facet since its growth rate is much smaller. The smaller surface energy of {111} (Refs. 6 and 13) also suggests the high probability of a dominant {111} faceting. But actually, a dominant {311} faceting was observed. We think that this is caused by a special growth kinetics which is favorable for {311} faceting on the Si(100) surface. Due to this growth kinetics, not the {111} but the {311} facet is initially formed at the SiO<sub>2</sub> side wall boundary. The {111} facet of a still slower growth rate is expected to appear as a

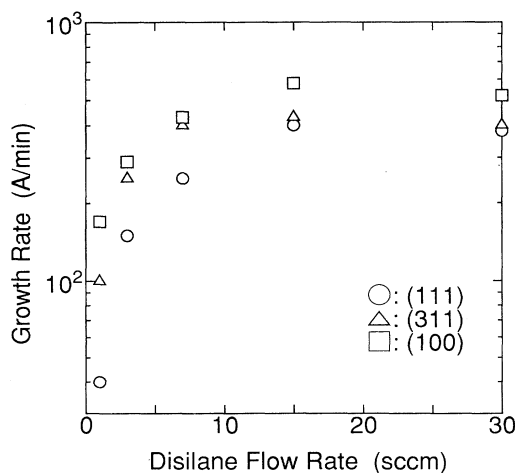


FIG. 6. UHV-CVD growth rate on Si(100), (311), and (111) surfaces. The growth rates were measured as a function of the disilane growth rate during the growth.

facet on the {311} surface, but only when the {311} facet grows large enough.

### B. Selective epitaxial growth on Si(100) vicinal surfaces

Just as in the case of Si(100) surfaces with no miscut, on vicinal Si(100) surfaces the selectively grown layers were observed to have a trapezoidal cross section. {311} facets appeared for the reason described in Sec. IV A. However, on vicinal surfaces, the top surface of the selectively grown layer changed from Si(100) vicinal to exactly Si(100) orientation. Here, we discuss the mechanism of this change.

As illustrated in Fig. 4, the left-side facet of the grown layer is larger than the right-side facet. Because facet growth is driven by nucleation of the migrating Si atoms of the top surface at the corner point, the larger facet on the left-hand side indicates net mass flow on the top surface from the right to the left. On the other hand, the vicinal surface is formed by introducing many steps into the Si(100) surface. The change from a vicinal to an exactly (100) surface is accomplished by reducing the step density. These two points introduce us to the following model. Generally, a Si adatom is readily incorporated at the step edges of a Si(100) surface. This produces step flow on Si(100) vicinal surfaces. However, at the corner point all the flowing steps are swallowed into the facet. Hence, during growth, the step density reduces and a net mass flow from right to left is accomplished by step growth toward the left side, as shown in Fig. 7. Therefore, the top surface change from vicinal to exactly (100)

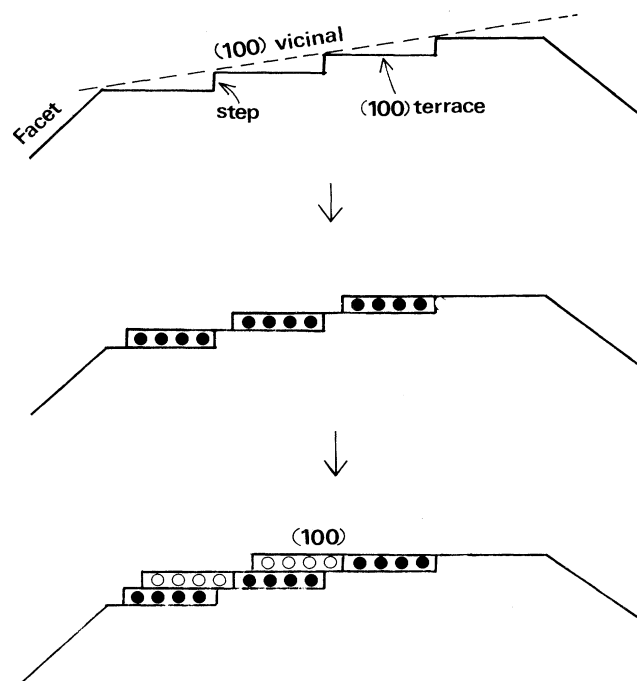


FIG. 7. A model of top surface orientation change in selective epitaxial growth on a Si(100) vicinal surface. Segments with closed and open circles indicate newly grown (100) terraces.

orientation is evidence that facet growth proceeds by swallowing the (100) terraces.

### C. A model of {311} faceting

As described in Sec. IV A, a growth kinetics seems to work favorably for the {311} faceting on Si(100) surface. Here, we propose a microscopic model for the {311} faceting. Our results on the vicinal surface clearly indicate that the steps of the layer-by-layer growing (100) surface is swallowed at the edge of the facet. The model is based on the rebonded termination of the step of the layer-by-layer growing Si(100) surface at the boundary between the (100) and the facet surfaces. In our model, the effect of H on the surface is neglected. In UHV-CVD, H exists on the growing surface. The H on the surface dangling bond may moderate the surface reconstruction. The surface energy is also expected to be changed by the adsorbed H. Hence, strictly speaking, our model is invalid for UHV-CVD, but is valid for MBE where H does not exist. However, in our experiment the growth is achieved with a small disilane flow rate. With a small flow rate, only a part of the surface is occupied by H, as described in Sec. IV A. Therefore, we expect that H has a minor effect on the growth kinetics in our study. Moreover, the large growing {311} faceting is observed not only in UHV-CVD, but also in the annealing of Si in UHV.<sup>6</sup> These suggest that the {311} faceting is an intrinsic character of Si crystal, and is not due to the H during UHV-CVD growth. With this respect, here we propose a microscopic mechanism of the {311} faceting, where the H effect is neglected.

Figure 8(a) illustrates the atomic structure of a growing film. In the initial stage, Si atoms are exposed only in the window area of the pattern [Fig. 8(a)]. Si atoms in the window form a characteristic dimer structure in the plane of the figure, as shown, to stabilize the surface energy. In the second stage of growth, Si atoms adsorb on the Si atoms already in the window, and form dimers which are perpendicular to the first dimers [Fig. 8(b)]. However, due to the lack of a Si atom in the underlying layer on the SiO<sub>2</sub> side, site "A" of the second layer cannot be occupied. Judging from the observed good selectivity, the SiO<sub>2</sub> surface has no stable adsorption site for Si,<sup>1</sup> and site "A" is energetically unfavorable for Si adsorption. As growth continues like this for two more layers [Figs. 8(c) and 8(d)], sites "B" and "C" also remain unoccupied and, as a result, a facet surface starts to appear at the SiO<sub>2</sub> boundary area. The key to {311} facet formation is the site "D." If this site remains unoccupied, the atomic structure becomes as in Fig. 8(d). A rebonded-type termination of the step<sup>14</sup> appears in the truncated step at the corner point. The rebonded Si atom "E" has bonds with one Si atom in the third layer and with two Si atoms in the second layer. By repeating the growth stages of (c) and (d), a {311} facet surface appears at the boundary as shown in Fig. 8(e). On the other hand, if the site "D" of Fig. 8(d) is occupied, the structure of Fig. 8(f) results. By repeating the growth stages of (c) and (f), a {111} facet appears as shown in Fig. 8(g).

The difference between the atomic structure of Fig.

8(d) for a {311} facet and (f) for a {111} facet comes from the truncation of the top layer's step at the corner point. If site "D" is unoccupied, rebonded-type step termination results, which reduces the number of dangling bonds, but a strain is built up. The step termination of Fig. 8(d) is just the same as the  $D_B$  step structure of Chadi's notation.<sup>14</sup> Chadi classified step structures on Si(100) as  $S_A$ - and  $S_B$ -type single-layer height steps and  $D_A$ - and  $D_B$ -type double-layer height steps.  $S_A$  is energetically more favorable than  $S_B$ , and  $D_B$  is more stable than  $D_A$ .<sup>14</sup> Using this notation, in the growth sequence of Figs. 8(c) and 8(d) for the {311} facet, the truncation at the corner point is  $S_A$  and  $D_B$ , respectively. Here, the  $D_B$  double-layer height step is caused by the rebonded atom "E." On the other hand, the truncation for the {111} facet alternates between  $S_A$  and  $S_B$  in Figs. 8(c) and 8(f), respectively. As Chadi pointed out,<sup>14</sup>  $D_B$  is much more stable than the  $S_A + S_B$  structure. The stability of  $D_B$  is due to the reduced number of dangling bonds by the rebonded atom. Therefore, we think that the {311} facet is fundamentally caused by the stability of  $D_B$ -type step termination of the growing Si(100) layers at the corner point.

Our model of {311} facet formation is supported by lattice images of the Si(311) surface using the high-resolution transmission electron microscope (HR-TEM) made by Gibson, McDonald, Unterwalt.<sup>15</sup> The cross-sectional lattice image and its simulation exactly agree with our atomic structure of the {311} facet in Fig. 8(e). However, the atomic structure in the direction perpendicular to the plane of Fig. 8 should be considered. In this direction,  $D_B$  step structure has long-range  $2 \times 1$  order. On the other hand,  $3 \times 2$  long-range order has been observed on the clean Si(311) surface.<sup>16-22</sup> In our experiment the small size of the pattern and shadowing by the SiO<sub>2</sub> sidewall did not allow us to observe the RHEED pattern from the facets, so the surface long-range order of the facet during and after growth are unknown. The facet surface structure during growth may differ from that of the static clean Si(311) surface. Actually, metastable  $5 \times 5$  structure has been reported during Si homoepitaxial growth on the Si(111)  $7 \times 7$  surface.<sup>23</sup> However, as the metastable structure of  $5 \times 5$  has a dimer-atom-stacking fault (DAS) structure similar to the stable Si(111)  $7 \times 7$  surface,<sup>24</sup> the growing structure of the {311} facet is expected to be at least similar to the  $3 \times 1$  or  $3 \times 2$  structure of the clean, static Si(311) surface.

Models of Si(311)  $3 \times 2$  surface structure that have been proposed by Ranke<sup>19</sup> are composed of rebonded atoms and additional five-atom clusters. A recent STM study also supports his model of Si(311)  $3 \times 2$ .<sup>21</sup> These studies indicate that the long-range order is basically caused by the arrangement of rebonded atoms. Rebonded atoms in a  $D_B$  step are arranged side by side along [110], whereas each rebonded atom of the Si(311) surface lacks any nearest-neighbor rebonded atoms, causing threefold order along [110]. Moreover, the positions of rebonded atoms in the neighboring [110] rows arrange so as not to overlap those in the other [110] rows. As described above, a rebonded atom reduces the number of dangling bonds and so is favorable from the viewpoint of electronic energy, but at the same time it introduces a local ten-

sile stress. On Si(100) vicinal surfaces, stress due to the rebonded atoms of each  $D_B$  step is relaxed on the neighboring wide terrace, thus stabilizing the  $D_B$  step. However, with increasing vicinal angles, the stress of  $D_B$  steps cannot be fully relaxed by the short terrace,<sup>19,25</sup> and the threefold arrangement of rebonded atoms of Si(311) appears. Hence, the Si(100) step at the facet corner basically tends to form a rebonded atomic termination, but to reduce the tensile stress a threefold long-range-ordered arrangement of the rebonded atoms may occur. Again, the TEM lattice image of the Si(311) surface<sup>15</sup> indicates that the rebonded atomic structure is the key to the (311) surface. We think that the rebonded atom termination of

the growing (100) terrace at the facet corner is the dominant driving force for {311} faceting.

## V. SUMMARY

Facets of a selectively grown Si epitaxial layer were studied on SiO<sub>2</sub> patterned Si(100) surfaces with miscut angles of 0°, 1°, 3°, and 4°. On all the surfaces, a {311} faceted Si(100) layer was observed. The {311} facets continued to grow until the (100) top layer disappeared. This means that the {311} facet is not caused by an equilibrium constraint such as achieving a small contact angle, but is closely related to the growth kinetics. Macroscopi-

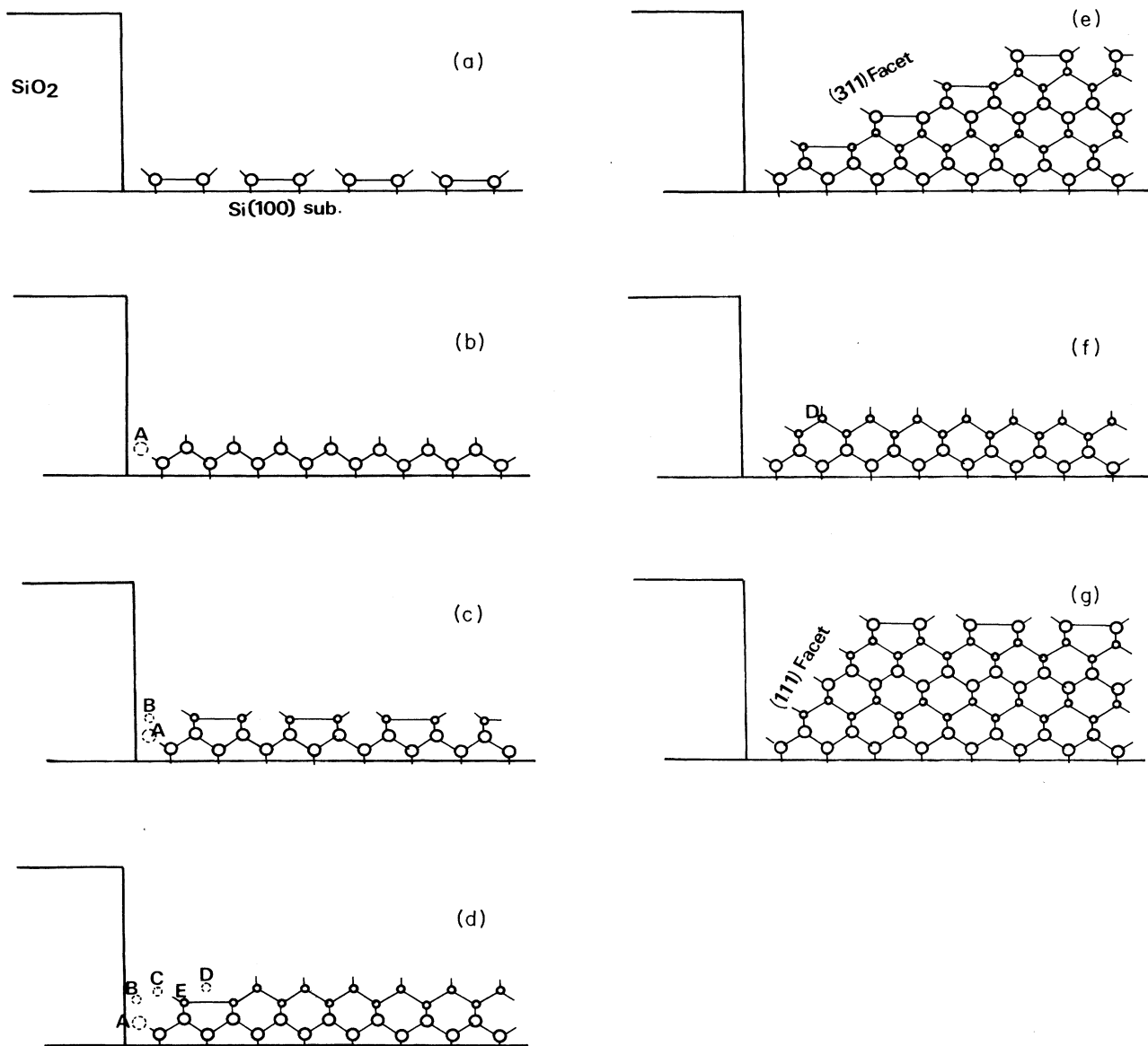


FIG. 8. A model of faceting in selective epitaxial growth of Si on a SiO<sub>2</sub> patterned Si(100) substrate with no miscut. Large circles indicate Si atoms in the plane of the figure. Small circles indicate Si atoms in the plane behind the large circles. Sharp lines denote chemical bonds. For other notation, see the text.

cally, the faceting is caused by the slower growth rate of the facet surface than that of the Si(100) surface. Actually, the growth rates of Si(311) and (111) surfaces are slower than that of Si(100) surface.

On Si(100) vicinal surfaces, the orientation of the selectively grown layer changes from Si(100) vicinal to an exactly (100) surface. This is due to the swallowing of steps at the facet corner. The swallowing of steps at the facet corner reduces the step density and makes the top surface flat during growth. On the base of the swallowing of

steps, we proposed a microscopic model to explain why the {311} is more favorable than the {111} facet. We think that the rebonded-type termination of the layer-by-layer growing of the (100) terrace at the facet edge is a key to the {311} faceting.

#### ACKNOWLEDGMENT

The authors thank Dr. D. Tweet for his critical reading of our manuscript.

- 
- <sup>1</sup>H. Hirayama, M. Hiroi, K. Koyama, T. Tatsumi, and M. Sato, in *Silicon Molecular Beam Epitaxy*, edited by J. C. Bean, S. S. Iyer, and K. L. Wang, MRS Symposia Proceedings No. 220 (Materials Research Society, Pittsburgh, 1991), p. 545.
- <sup>2</sup>H. Hirayama, M. Hiroi, K. Koyama, and T. Tatsumi, *Appl. Phys. Lett.* **56**, 1107 (1990).
- <sup>3</sup>M. Hiroi and T. Tatsumi, *J. Cryst. Growth* **120**, 279 (1992).
- <sup>4</sup>F. Sato, H. Takemura, T. Tashiro, H. Hirayama, M. Hiroi, and M. Nakamae, *IEDM Tech. Dig.* **90**, 607 (1990).
- <sup>5</sup>M. Hiroi and H. Hirayama (unpublished).
- <sup>6</sup>D. J. Eaglesham, A. E. White, L. C. Feldman, N. Moriya, and D. C. Jacobson, *Phys. Rev. Lett.* **70**, 1643 (1993).
- <sup>7</sup>B. A. Joyce, J. H. Neave, and B. E. Watts, *Surf. Sci.* **15**, 1 (1969).
- <sup>8</sup>G. R. Booker and B. A. Joyce, *Philos. Mag.* **14**, 301 (1966).
- <sup>9</sup>D. J. Eaglesham, G. Higashi, and M. Cerullo, *Appl. Phys. Lett.* **59**, 685 (1991).
- <sup>10</sup>D. J. Eaglesham, F. C. Unterwald, and D. C. Jacobson, *Phys. Rev. Lett.* **70**, 966 (1993).
- <sup>11</sup>N. Ohshima, Y. Koide, K. Itoh, S. Zaima, and Y. Yasuda, *Appl. Surf. Sci.* **48/49**, 69 (1991).
- <sup>12</sup>H. Hiroi, M. Koyama, T. Tatsumi, and H. Hirayama, *Appl. Phys. Lett.* **60**, 1723 (1992).
- <sup>13</sup>D. M. Bird, L. J. Clarke, R. D. King-Smith, M. C. Payne, I. Stich, and A. P. Sutton, *Phys. Rev. Lett.* **69**, 3785 (1992).
- <sup>14</sup>D. J. Chadi, *Phys. Rev. Lett.* **59**, 1691 (1987).
- <sup>15</sup>J. M. Gibson, M. L. McDonald, and F. C. Unterwald, *Phys. Rev. Lett.* **55**, 1765 (1985).
- <sup>16</sup>B. Z. Olshanetsky and V. I. Mashanov, *Surf. Sci.* **111**, 414 (1981).
- <sup>17</sup>U. Myler and K. Jacobi, *Surf. Sci.* **220**, 353 (1989).
- <sup>18</sup>Y.-N. Yang, E. D. Williams, R. L. Park, N. C. Bartlet, and T. L. Einstein, *Phys. Rev. Lett.* **64**, 2410 (1990).
- <sup>19</sup>W. Ranke, *Phys. Rev. B* **41**, 5243 (1990).
- <sup>20</sup>U. Myler, P. Althainz, and K. Jacobi, *Surf. Sci.* **251/252**, 607 (1991).
- <sup>21</sup>J. Knall, J. B. Pethica, J. D. Todd, and J. H. Wilson, *Phys. Rev. Lett.* **66**, 1733 (1991).
- <sup>22</sup>K. Jacobi and U. Myler, *Surf. Sci.* **284**, 223 (1993).
- <sup>23</sup>H. Nakahara and A. Ichimiya, *Surf. Sci.* **241**, 124 (1991).
- <sup>24</sup>K. Takayanagi, Y. Tanishiro, M. Takahashi, and S. Takahashi, *J. Vac. Sci. Technol. A* **3**, 1502 (1985).
- <sup>25</sup>E. Schroder-Bergen and W. Ranke, *Surf. Sci.* **259**, 323 (1991).

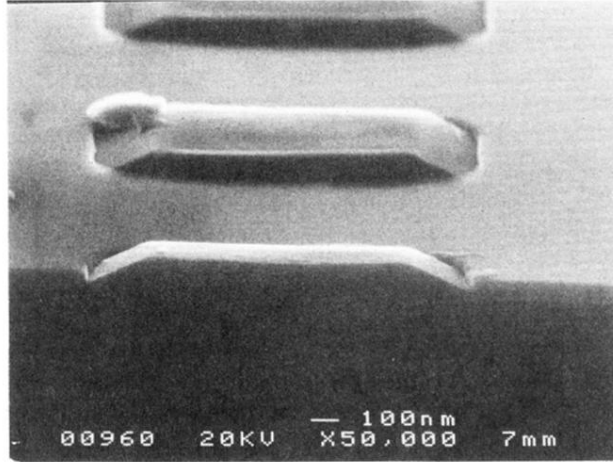


FIG. 1. SEM image of a selectively grown Si layer on the SiO<sub>2</sub> patterned Si(100) surface with no miscut.

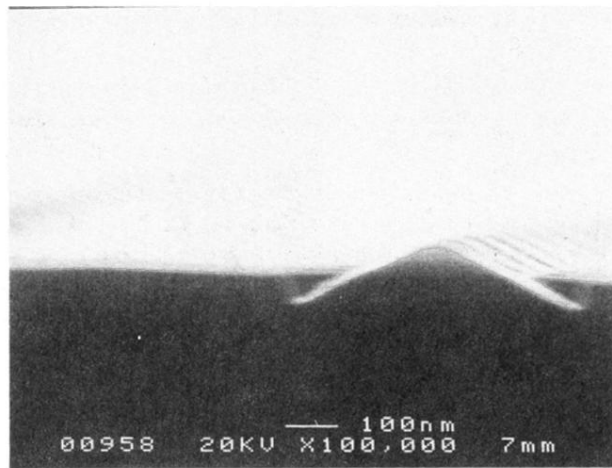


FIG. 2. SEM image of a selectively grown Si layer on the SiO<sub>2</sub> patterned Si(100) surface with no miscut, in which the {311} facets grew until the top (100) surface disappeared.

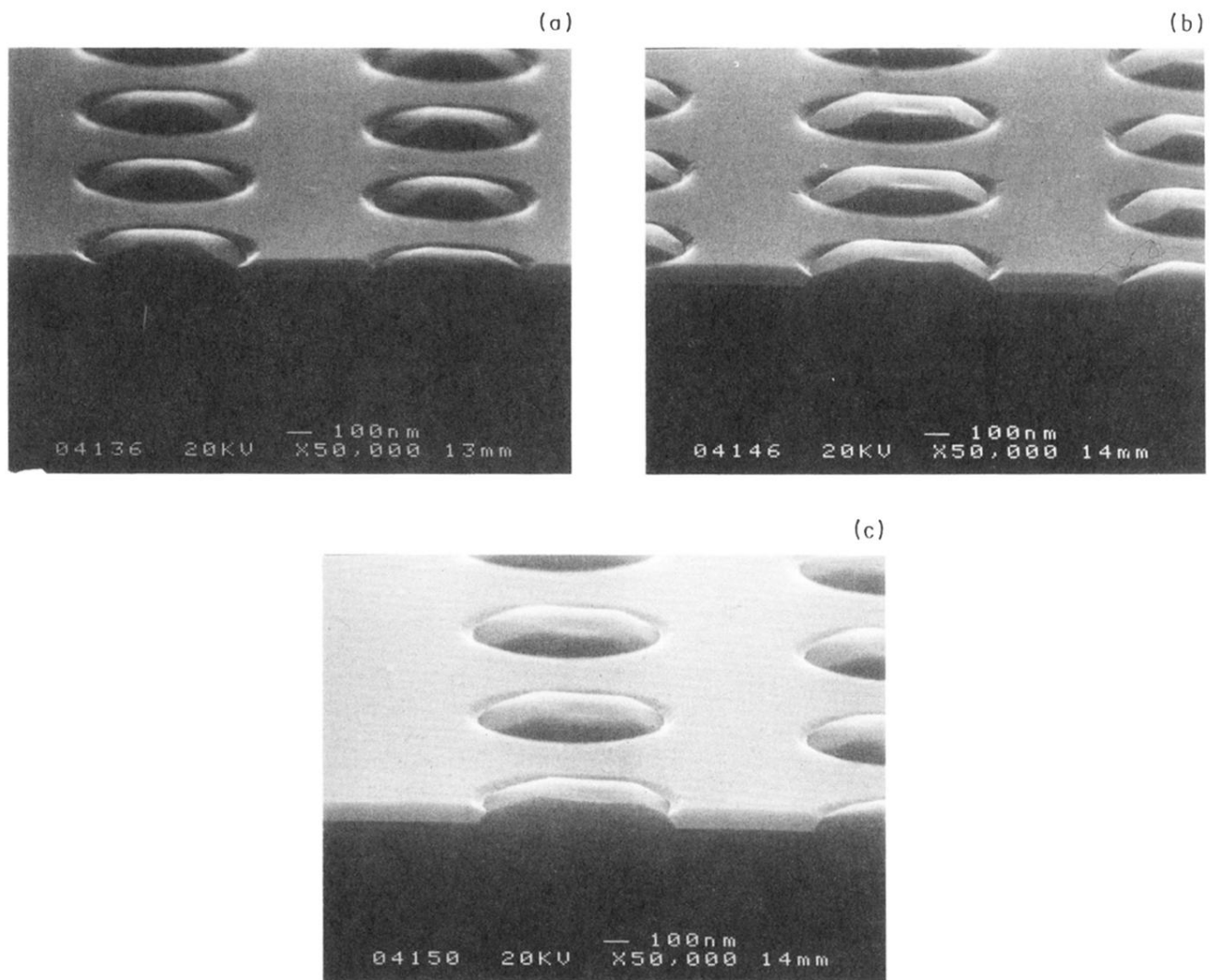


FIG. 3. SEM images of selectively grown Si layers on SiO<sub>2</sub> patterned Si(100) vicinal surfaces with miscut angles of (a) 1°, (b) 3°, and (c) 4° off.